Desalination and Water Treatment
www.deswater.com

doi: 10.1080/19443994.2015.1132474

57 (2016) 21925–21938
October

Taylor & Francis
Taylor & Francis Group

Adsorption kinetics and isotherms for the removal of nickel ions from aqueous solutions by an ion-exchange resin: application of two and three parameter isotherm models

N.S. Yousef*, Rania Farouq, Riham Hazzaa

Faculty of Engineering, Petrochemical Department, Pharos University, Canal El, Mahmoudeya St. Semouha, Alexandria, Egypt, Tel. +20 3 01006741024, +20 3 3877200, +20 3 3877400, +20 3 3877212, +20 3 3877214; emails: nohaysf@gmail.com (N.S. Yousef), rania.farouq@pua.edu.eg (R. Farouq), riham17@yahoo.com (R. Hazzaa)

Received 17 October 2014; Accepted 1 December 2015

ABSTRACT

The capacity of a strong cation-exchange resin for removal of nickel from aqueous solutions was investigated under different conditions such as contact time, initial nickel ion concentration, stirring speeds, solution pH, and resin dose. The equilibrium isotherm data were analyzed using Langmuir, Freundlich, Temkin, Elovich, Fowler–Guggenheim, Kiselev, Hill–de Boer, Jovanovic, Hill, and Koble–Corrigan isotherms. Correlation coefficients indicated the following order to fit isotherms: Langmuir > Koble–Corrigan > Freundlich > Hill > Jovanovic > Temkin > Hill–de Boer > Fowler–Guggenheim > Kiselev > Elovich. On the basis of the lowest values of the four error functions studied, Hill model provided the best correlation for the experimental data. The kinetic data were analyzed using pseudo-first-order, pseudo-second-order, and Elovich model. Intra-particle diffusion model and the liquid film diffusion model were used to investigate the adsorption mechanism. Kinetic studies showed that the adsorption of Ni^{2+} ions onto ion-exchange resin followed Elovich kinetic model, and indicates that the intra-particle diffusion controls the rate of adsorption. Furthermore, separation factors and distribution coefficients of nickel were calculated.

Keywords: Ion exchange; Nickel(II); Equilibrium isotherms; Kinetic models; Diffusion models; Error analysis

1. Introduction

Heavy metals can be distinguished from other pollutants, since they are not biodegradable and can lead to accumulation in living organisms, causing various diseases and disorders, even if the metal concentration in water is relatively low [1,2]. The metals of most immediate concern are cadmium, chromium, cobalt, copper, lead, nickel, mercury, and zinc. The effluents from metal finishing processes may contain up to 10 mg/L of copper, chromium, nickel, and zinc [3]. Nickel is a toxic heavy metal that is widely used in the production of stainless steel, electroplating, zinc base casting, and storage battery industries [4]. The current technologies for the removal of nickel include chemical precipitation, electro dialysis, membrane filtration, and activated carbon adsorption [5–7]. However, there is a need to develop cost-effective technologies for treating the wastewater that reduce metal ion concentrations to environmentally acceptable levels [8,9].

---

*Corresponding author.

Adsorption or biosorption have been found to be very effective recently due to its properties which can be used in wastewater treatments with the advantages of simplicity in operation, lowcost, and insensitivity to toxic substances compared to other separation methods [10,11]. Adsorbents like cassava peel, *Cymbopogon citratus* (lemon grass), *Bacillus laterosporus* (MTCC 1628), cashew nut shell, rice husk, activated carbon, chitosan, zeolite, and fly ash have been proven to be useful for the removal of nickel ion from wastewater [12–18]. However, ion-exchange technology is more efficient in ion removal from the wastewater. Ion exchange can remove approximately about 97% of nickel ion from wastewater [19–21].

Adsorption isotherms are used to describe how heavy metal ions interact with adsorbent materials, so modeling of adsorption isotherm data is important for predicting and comparing adsorption performance: such as the calculation of the capacities of adsorbents [22–28]. Two, three, and even four-parameter isotherm models are developed for modeling adsorption data. Langmuir and Freundlich models are used to describe the adsorption isotherm and are usually preferred because spite of their simplicity, they can be easily linearized. In spite of this, few three parameter models such as Redlich–Peterson and Sips model were also used to describe the adsorption isotherm with high accuracy [29–32]. When adsorption is concerned, thermodynamic and kinetic aspects should be involved to know more details about its performance and mechanisms [33,34]. Linear least-squares method is widely used for the determination of the isotherm parameters and the most fitted model with the magnitude regression correlation coefficients that close to unity. Nevertheless, nonlinear optimization provides a mathematically rigorous method for determining isotherm parameter values with a number of error analysis techniques [22,35].

The present work aims to examine the sorption properties of a strong cationic exchange resin towards nickel ion. The influence of experimental parameters such as contact time, adsorbent dose, stirring speed, solution pH, and initial nickel concentrations were studied at 25°C. The kinetic and equilibrium data of adsorption studies were processed to understand the adsorption mechanism of the nickel ions onto the cationic-exchange resin.

2. Materials and methods

2.1. Materials

All the chemicals used were of analytical reagent (AR) grade. IR 120H strong acid cationic-exchange resin was used. A stock solution of nickel (1,000 mg/L) was prepared by dissolving $NiCl_2{\cdot}6H_2O$ in double distilled water. The concentration range of nickel prepared from stock solution varied between 500 and 1,000 mg/L.

2.2. Methods

The concentrations of nickel in the solutions before and after removal by the cationic resin were determined by atomic absorption spectrometer. The solution pH was adjusted by dropwise of 0.1 M NaOH or 0.1 M HCl solutions and measured by pH meter.

2.3. Adsorption isotherms

Batch adsorption experiments were carried out at the room temperature of 25°C in Erlenmeyer flasks (250 mL) by adding 0.5–4 g resin and 100 ml of nickel chloride solution of specific concentration. The concentration of Ni^{2+} solution was varied from 500 to 1,000 mg/L.

The samples were stirred using a mechanical stirrer for a contact time ranging from 5 to 150 min. Stirring speed varied from 50 to 1,300 rpm. After each experiment, the contents were filtered through a filter paper neglecting the first 5 ml of the filtrate in order to saturate the filter paper with nickel chloride solution. Concentrations of nickel ions in the filtrate were then determined by atomic absorption spectrophotometer. All the experiments were performed in duplicates. The percentage removal of nickel from the aqueous solution was calculated according to the following equation:

$$\text{Removal}\,\% = \frac{C_o - C_e}{C_o} \times 100 \tag{1}$$

The amount of nickel adsorbed at equilibrium, q_e (mg/g), was calculated by the following mass balance relationship:

$$q_e = C_o - C_e \times \frac{V}{m} \tag{2}$$

where C_o and C_e are the initial and equilibrium liquid-phase concentrations of nickel, respectively (mg/L), V the volume of the solution (L), and m is the weight of the adsorbent used (g).

3. Results and discussions

3.1. Effect of contact time

Adsorption of nickel was determined at given contact time for six different initial Ni^{2+} concentrations of

500, 600, 700, 800, 900, and 1,000 mg/L. IR 120 H resin was used as an adsorbent in bench scale studies. Fig. 1 shows that the percentage removal of nickel from the aqueous solution by resin is higher at the beginning of the adsorption process. This is probably due to larger surface area of the resin available at the beginning for adsorption of Ni^{2+} ions. As the surface adsorption sites become exhausted, the uptake rate is controlled by the rate at which the adsorbate is transferred from the exterior to the interior sites of the adsorbent particles. The maximum percentage removal of nickel by resin was attained at about 40 min of shaking time for all concentrations.

3.2. Effect of initial concentration

The initial concentration of metal ion provides an important driving force to overcome all mass transfer resistances of metal ions between the aqueous and solid phases [36]. The sorption of Ni^{2+} ions onto various adsorbents was carried out at different initial Ni^{2+} ion concentrations ranging from 500 to 1,000 mg/L. Fig. 2 shows that by increasing the concentration gradually, there is a decrease in the percentage removal of nickel ions from the aqueous solution. As the ratio of sportive surface to ion concentration decreased with increasing metal ion concentration and so metal ion removal was reduced. At low initial concentration of metal ions, more binding sites are available. But as the concentration increases, the number of ions competing for available binding sites in the biomass increased [37].

3.3. Effect of adsorbent dose

The effect of the adsorbent dose was studied by varying the sorbent amounts from 0.5 to 4 g/100 ml. This effect was studied for initial concentrations of nickel (500, 600, and 800 mg/L). Fig. 3 reveals that the percentage removal of nickel ion from aqueous solution increases by increasing the adsorbent dose of the cation resin. The number of available adsorption sites increases by increasing the adsorbent dose and this results in an increase in removal efficiency. As expected, the equilibrium concentration decreases with increasing adsorbent doses for a given initial nickel concentration [38].

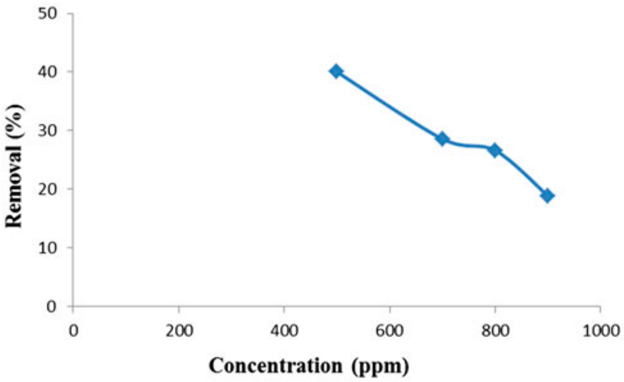

Fig. 2. Effect of initial nickel concentration on removal of Ni^{2+} ions.

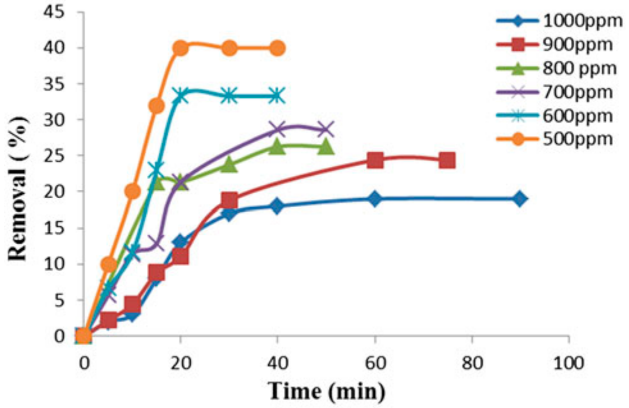

Fig. 1. Effect of contact time on removal of Ni^{2+} ions.

3.4. Effect of stirring speed

Stirring is an important parameter in adsorption phenomena, influencing the distribution of the solute in the bulk solution and the formation of external boundary film. Fig. 4 shows the adsorption rate of Ni^{2+} ion using resin at different stirring speeds (50, 250, 565, and 1,300 rpm), and different concentrations

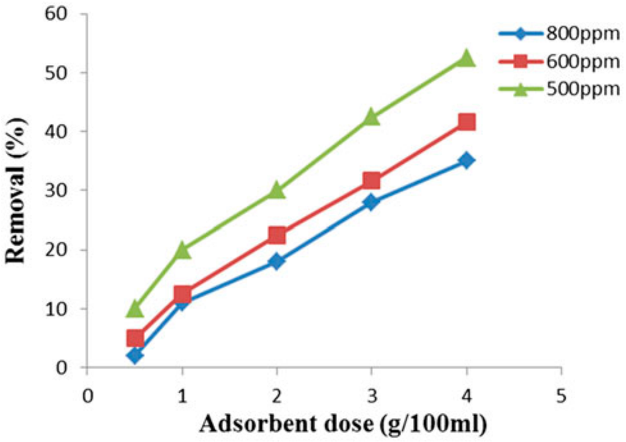

Fig. 3. Effect of adsorbent dose on removal of Ni^{2+} ions.

(500, 800, and 1,000 mg/L) within contact time of 60 min. It is clear from Fig. 4 that with increasing stirring speed, the percentage removal of nickel ion increases until stirring speed of 250 rpm, and then decreases. The increasing in ion-exchange capacity can be explained by the fact that increasing stirring speed reduces the film boundary layer surrounding ions, thus increasing the external film transfer coefficient, and hence the adsorption capacity. Similar result was also reported in the literature [39]. On the other hand, high stirring speeds above 250 rpm can cause desorption of Ni^{2+} ions metal since the metal ions leave the binding sites and transfer to the solution, resulting in low adsorption capacity and accordingly low percentage removal.

3.5. Effect of pH

The pH of solution is one of the most important parameters controlling uptake of heavy metals from aqueous solution. The effect of pH on the sorption of Ni^{2+} ions was tested at different pH values (2.0–9.0). The results indicated that the maximum uptake of Ni^{2+} ions occurred at initial pH of 5.0 for the resin. The adsorption capacity of the resin increased with the increase in pH of the aqueous solution. This can be explained on the basis of decrease in competition between protons (H^+ ions)/(Na^+) and metal cations (Ni^{2+} ions) for the functional group ($-SO_3^-$) for the strong acid resin, resulting in a lower electrostatic repulsion between the surface of the adsorbent and Ni^{2+} ions [40]. After pH 5, it decreases very slowly up to pH 9. The decrease in adsorption at higher pH may be attributed to the hydrolysis of Ni^{2+} in the solution, and therefore the separation may not be due to adsorption.

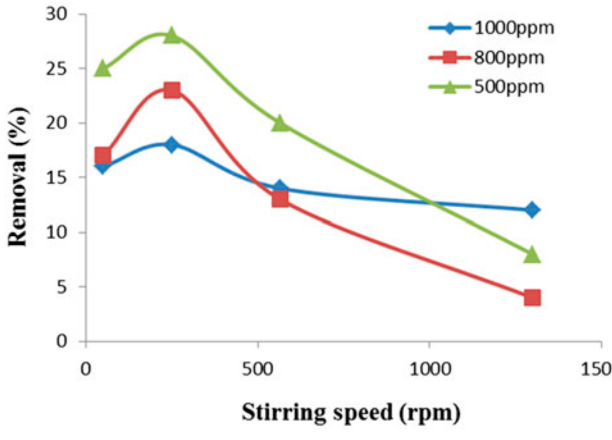

Fig. 4. Effect of stirring speed on removal of Ni^{2+} ions.

3.6. Adsorption isotherms

Adsorption isotherm expresses the relationship between the amounts of adsorbate removed from the liquid phase by unit mass of adsorbent at a constant temperature. The parameters of equilibrium isotherms often give useful information on sorption mechanism, surface properties affinity of the adsorbent. It is therefore important to determine the most suitable correlation of equilibrium curves in order to optimize the conditions for designing adsorption systems [41].

In this study, the Langmuir, Freundlich, Temkin, Elovich, Fowler–Guggenheim, Kiselev, Hill–de Boer, Jovanovic, Hill, and Koble–Corrigan isotherms were tested to analyze the equilibrium data, and the results are shown in Fig. 5.

The Langmuir isotherm is used to describe adsorption phenomena and is based on the assumption that up take occurs on a homogenous surface by monolayer sorption without interaction between adsorbed molecules. The linear form of the Langmuir isotherm equation can be expressed as [42]:

$$\frac{1}{q_e} = \frac{1}{K_L \times q_m} \times \frac{1}{C_e} + \frac{1}{q_m} \tag{3}$$

where q_m is the maximum monolayer adsorption capacity (mg/g) and K_L is the Langmuir constant which is related to the heat of adsorption (L/mg). From Table 1, the correlation coefficient (R^2) is very high (0.972), indicating a best fit of the monolayer Langmuir isotherm to the adsorption of Ni^{2+} by the resin. The monolayer adsorption capacity for Ni(II) removal was 27.868 mg/g as shown in Table 1.

Essential features of the Langmuir isotherm can be expressed in terms of dimensionless separation factor (R_L) given by [43]:

$$R_L = \frac{1}{1 + K_L \times C_o} \tag{4}$$

The value of separation factor R_L indicates either the adsorption isotherm to be unfavorable ($R_L > 1$), favorable ($0 < R_L > 1$), linear ($R_L = 1$), or irreversible ($R_L = 0$). The values of R_L were in the range of 0–1 (in range of 0.644–0.783), indicating the favorable adsorption of Ni^{2+} on the resin.

The Freundlich sorption isotherm [44], is one of the most widely used mathematical descriptions, usually fits the experimental data over a wide range of concentrations. This isotherm gives an expression encompassing the surface heterogeneity, the exponential distribution of active sites and their energies; it is expressed by the following equation:

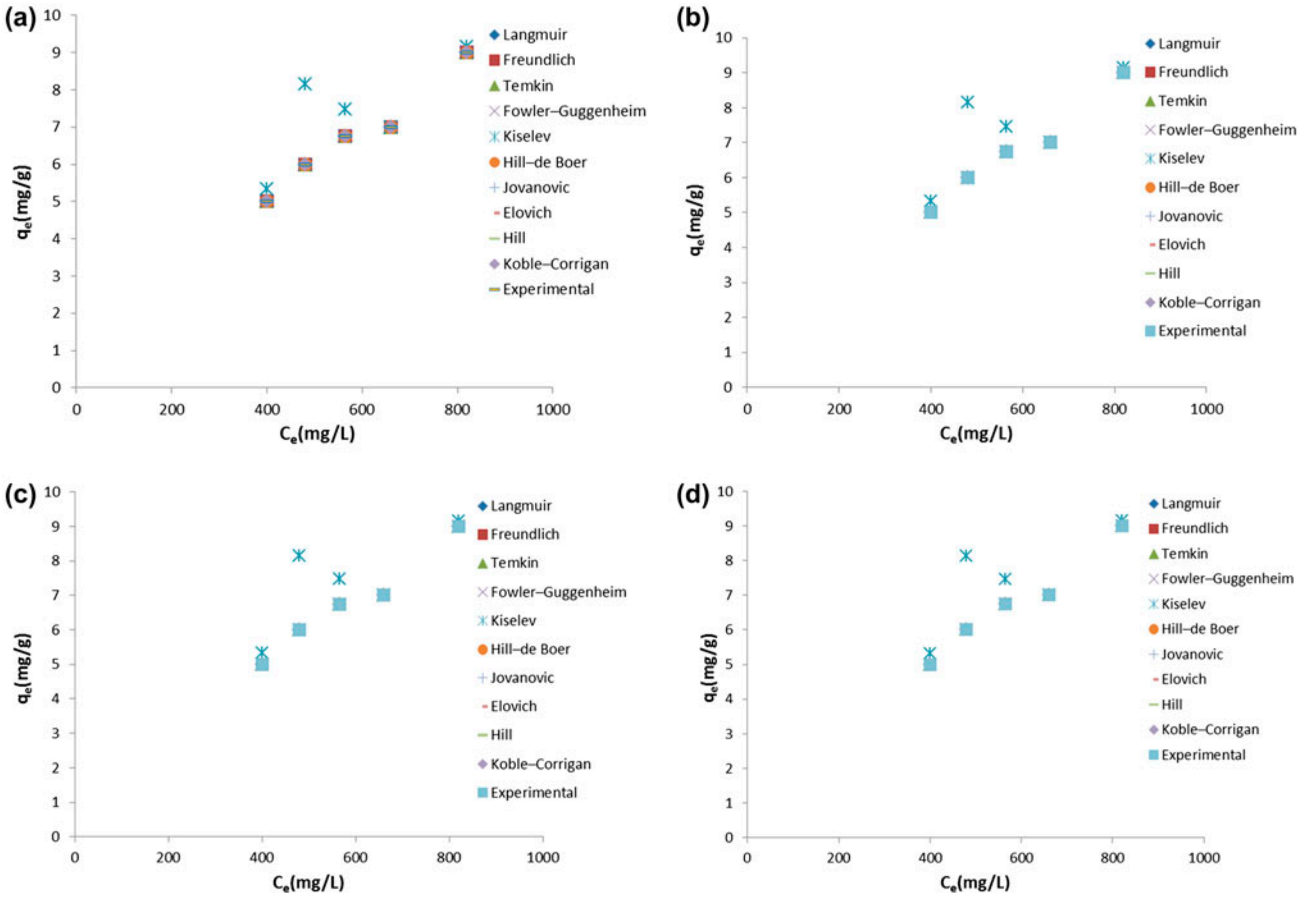

Fig. 5 Comparison of experimental and predicted isotherms of Ni^{2+} sorption based on error function of HYBRID (a), ARE (b), EABS (c), and MPSD (d), cation-exchange resin.

$$\log q_e = \log K_F + \frac{1}{n_f} \log C_e \tag{5}$$

where K_F (mg/g) $(mg/L)^{1/n}$, and n_f are Freundlich adsorption constants related to the adsorption capacity and intensity of the adsorbents, respectively. The constants were determined by the linear plot of log q_e vs. log C_e.

As can be seen from Table 1 the value of the correlation coefficient (R^2) was 0.969 for Ni^{2+} ions, which is a high value and very close to that of Langmuir isotherm. Furthermore, if the value of n_f lies between 1 and 10, it indicates a favorable adsorption [45]. The value of n_f obtained was 1.38, indicating a favorable adsorption process.

The Temkin isotherm model unlike the Langmuir and Freundlich isotherms takes into account the interactions between adsorbents and metal ions to be adsorbed and is based on the assumption that the free energy of sorption is a function of the surface coverage [46]. The linear form of the Temkin isotherm model is expressed by the following equation [47]:

$$q_e = B \ln A_T + B \ln C_e \tag{6}$$

where $B = RT/b_T$, T is the temperature (K), R is the ideal gas constant (8.314 J/mol K), and A_T and b_T are constants. The constant B is related to the heat of adsorption and A is the equilibrium binding constant (L/mg), corresponding to the maximum binding energy. The plot of q_e vs. ln C_e enables the determination of A_T and B. The value of the regression coefficient R^2 was 0.952 as seen from Table 1 which is lower than that of the both Freundlich and Langmuir isotherm models.

The equation defining the Elovich [48] model is based on a kinetic principle assuming that the adsorption sites increase exponentially with adsorption, which implies a multilayer adsorption. It is expressed by the relation:

Table 1
Isotherm Constants for Ni^{2+} ions adsorption onto cation-exchange resin

Isotherm model	Isotherm parameters	R^2 of isotherm model
Langmuir	$q_m = 27.8682$ $K_L = 0.00055$	0.972
Freundlich	$K_F = 0.0519$ $n_f = 1.3078$	0.969
Temkin	$A_T = 0.00646$ $B = 476.9058$ $b_T = 5.195$	0.952
Elovich	$q_m = 26.2215$ $K_E = 0.000576$	0.556
Fowler–Guggenheim	$W = -34{,}032$ $K_{FG} = 2.25 \times 10^{-6}$	0.842
Kiselev	$k_1 = -0.0017$ $kn = -6.61781$	0.749
Hill–de Boer	$K_{1H} = 2.14810^{-6}$ $K_2 = 71822.53$	0.856
Jovanovic	$K_j = -0.0013$ $q_m = 3.1004$	0.963
Hill	$K_D = 15042.753$ $n_H = 0.7831$ $q_{SH} = 701.53$	0.968
Koble–Corrigan	$a = 0.052626$ $b = 1.727 \times 10^{-6}$ $n_{(k\text{-}c)} = 0.873224$	0.972

$$\frac{q_e}{q_m} = K_E C_e \, e^{-\frac{q_e}{q_m}} \tag{7}$$

where K_E is the Elovich equilibrium constant (L/mg) and q_m is the Elovich maximum adsorption capacity (mg/g). If the adsorption obeys Elovich equation, Elovich maximum adsorption capacity, and Elovich constant can be calculated from the slopes and the intercepts of the plot $\ln(q_e/C_e)$ vs. q_e. As shown from Table 1, the value of the regression coefficient R^2 was 0.556 which is very low; therefore the adsorption of nickel onto cation resin does not fit the Elovich isotherm.

Fowler–Guggenheim [49] derived an isotherm equation which takes the lateral interaction of the adsorbed molecules into account. It has the following explicit form:

$$K_{FG} C_e = \frac{\theta}{1-\theta} e^{\frac{2\theta W}{RT}} \tag{8}$$

where K_{FG} is the Fowler–Guggenheim equilibrium constant (L/mg), θ the fractional coverage, R the universal gas constant (kJ/mol K), T the temperature (K), and W is the interaction energy between adsorbed molecules (kJ/mol). Fowler–Guggenheim equation is one of the simplest equations allowing for the lateral interaction. The heat of adsorption varies linearly with loading. If the interaction between the adsorbed molecules is attractive (that is W is positive), the heat of adsorption will increase with loading and this is due to the increased interaction between adsorbed molecules as the loading increases. This means that if the measured heat of adsorption shows an increase with respect to loading, it indicates the positive lateral interaction between adsorbed molecules. However, if the interaction among adsorbed molecules is repulsive (that is W is negative), the heat of adsorption shows a decrease with loading. When there is no interaction between adsorbed molecules (that is $W = 0$), this Fowler–Guggenheim equation will reduce to the Langmuir equation. As shown from Table 1, the value of the regression coefficient R^2 was 0.842, which is lower than that of Langmuir, Freundlich, and Temkin isotherms. The value of W was −34,032, indicating repulsive interaction among adsorbed molecules, and showing a decrease in the heat of adsorption with loading.

The equation of Kiselev [50] known as the adsorption isotherm in localized monomolecular layer is expressed by:

$$K_{1\mathrm{K}} C_{\mathrm{e}} = \frac{\theta}{(1-\theta)(1+k_n\theta)} \tag{9}$$

where $K_{1\mathrm{K}}$ is the Kiselev equilibrium constant (L/mg), θ the fractional coverage, and k_n is the constant of complex formation between adsorbed molecules. A plot of $1/C_{\mathrm{e}}(1-\theta)$ vs. $1/\theta$ gives the slope k_1, and intercept $k_1 \times k_n$. The value of the regression coefficient R^2 was 0.7496 as seen from Table 1, which is lower than that of the Langmuir, Freundlich, Temkin, and Fowler–Guggenheim isotherm models.

Hill–de Boer model [51,52] describes the mobile adsorption and lateral interaction among adsorbed molecules by the equation:

$$K_{1\mathrm{H}}\, C_{\mathrm{e}} = \frac{\theta}{1-\theta_{\mathrm{H}}} e^{\left(\frac{\theta_{\mathrm{H}}}{1-\theta_{\mathrm{H}}}\right)-\left(\frac{K_2\theta_{\mathrm{H}}}{RT}\right)} \tag{10}$$

where $K_{1\mathrm{H}}$ is the Hill–de Boer constant (L/mg), K_2 is the energetic constant of the interaction between adsorbed molecules (J/mol). A positive K_2 value indicates the attraction between adsorbed species and a negative value means repulsion. The apparent affinity is increased with loading when there exist the attraction between adsorbed species and it is decreased with loading when there is repulsion among the adsorbed species. When there is no interaction between adsorbed molecules (i.e. $K_2 = 0$), the Hill–de Boer equation will be reduced to the Volmer equation. The value of the regression coefficient R^2 was 0.8559 as seen from Table 1, which is lower than that of the Langmuir, Freundlich, and Temkin isotherm models. The value of K_2 was 71822.53 which is a positive value, indicating attraction between adsorbed species, which results in increasing affinity with loading.

An adsorption surface assumption considered in Jovanovic isotherm model [53] is similar to that considered by Langmuir. It corresponds to another approximation for monolayer localized adsorption without lateral interactions. This model is similar to that of Langmuir model, except that the allowance is made in the former for the surface binding vibrations of an adsorbed species. This model is shown by using the following nonlinear relationship:

$$q_{\mathrm{e}} = q_{\mathrm{m}}(1 - e^{K_{\mathrm{j}}C_{\mathrm{e}}}) \tag{11}$$

where K_{j} is the Jovanovic isotherm constant (L/mg), q_{m} is the maximum adsorption capacity in Jovanovic model (mg/g). As shown form Table 1, the value of the regression coefficient R^2 was 0.963, which is lower than that of Langmuir, and Freundlich, but higher than that of Temkin, Hill–de Boer, Fowler–Guggenheim, Kiselev, and Elovich isotherm models. Hill equation [54], from the non-ideal competitive adsorption [55] model, and postulated to explain about the binding of different species onto homogeneous substrates. The model assumes that adsorption process as a cooperative phenomenon, with the ligand binding ability at one site on the macromolecule, may influence the different binding sites on the same macromolecule [56]. It is described by the following equation:

$$q_{\mathrm{e}} = \frac{q_{\mathrm{sH}} \times C_{\mathrm{e}} \times n_{\mathrm{H}}}{K_{\mathrm{D}} + C_{\mathrm{e}} \times n_{\mathrm{H}}} \tag{12}$$

where q_{sH} is the Hill isotherm maximum uptake saturation (mg/L), K_{D} is the Hill constant, n_{H} is the Hill cooperativity coefficient of the binding interaction. As seen from Table 1, the value of the regression coefficient R^2 was 0.968 which is lower than that of Langmuir, and Freundlich models, and higher than that of Jovanovic, Temkin, Hill–de Boer, Fowler–Guggenheim, Kiselev, and Elovich isotherm models.

Koble–Corrigan model [57] is a three-parameter empirical model based on the combination of both the Langmuir and Freundlich isotherm equations representing in one nonlinear equation of the equilibrium adsorption data. The model is commonly expressed by:

$$q_{\mathrm{e}} = \frac{aC_{\mathrm{e}}^{n_{(k-c)}}}{1 + bC_{\mathrm{e}}^{n_{(k-c)}}} \tag{13}$$

where a ($\mathrm{L}^n\ \mathrm{mg}^{1-n}/\mathrm{g}$), b $(\mathrm{L/mg})^n$, and $n_{(k\text{–}c)}$ are the Koble–Corrigan parameters. This model is generally applied for heterogeneous sorbent surface [58].

As shown in Table 1, the value of the regression coefficient R^2 was 0.972, which is lower than that of Langmuir isotherm, and higher than all the other isotherm models.

3.7. Error functions

In this study, four different error functions were examined and in each case the isotherm parameters were determined by minimizing the respective error function across the concentration range studied using the Solver add-in with Microsoft Excel. If the deviation of predicted data from experimental data is small, the function value will be a small number, and vice versa. The error functions studied were detailed in the following sections.

3.7.1. The hybrid fractional error function

This error function was developed by Porter et al. [59] in an attempt to improve the fit of the sum of the squares of the errors at low concentrations by dividing it by the measured value. It also includes the number of degrees of freedom of the system, the number of data points, n, minus the number of parameters, p, of the isotherm equation as a divisor.

$$\frac{100}{n-p}\sum_{i=1}^{n}\frac{\left(q_{\mathrm{e,i,meas}}-q_{\mathrm{e,i,cal}}\right)^2}{q_{\mathrm{e,i,meas}}} \tag{14}$$

where $q_{\mathrm{e,i,meas}}$ and $q_{\mathrm{e,i,cal}}$ are the values of q_{e} (mg/g) experimental equilibrium measurement, and calculated by isotherm model, respectively.

3.7.2. The average relative error

This error function [60] attempts to minimize the fractional error distribution across the entire concentration range.

$$\frac{100}{n}\sum_{i=1}^{n}\left|\frac{q_{\mathrm{e,i,cal}}-q_{\mathrm{e,i,meas}}}{q_{\mathrm{e,i,meas}}}\right| \tag{15}$$

3.7.3. The sum of the absolute errors

This approach is similar to the sum of the squares of the errors. Isotherm parameters determined using this error function would provide a better fit as the magnitude of the error increase, biasing the fit towards the high concentration data:

$$\sum_{i=1}^{n}\left|q_{\mathrm{e,i,cal}}-q_{\mathrm{e,i,meas}}\right| \tag{16}$$

3.7.4. Marquardt's percent standard deviation

This error function [61] was used previously by a number of researchers in the field [62]. It is similar in some respects to a geometric mean error distribution modified according to the number of degrees of freedom of the system:

$$100\sqrt{\frac{1}{n-p}\sum_{i=1}^{n}\left(\frac{q_{\mathrm{e,i,meas}}-q_{\mathrm{e,i,cal}}}{q_{\mathrm{e,i,meas}}}\right)} \tag{17}$$

The data obtained from different error functions were summarized in Table 2, and Fig. 5. On the basis of the lowest values of hybrid fractional error function (HYBRID), average relative error (ARE), sum of the absolute errors (EABS), and Marquardt's percent standard deviation (MPSD), Hill model provided the best correlation for the experimental data.

3.8. Adsorption kinetics

The adsorption kinetics is one of the most important data used to understand the mechanism of the adsorption and to assess the performance of the adsorbents. Different kinetic models including pseudo-first-order, pseudo-second-order, and Elovich model were applied for the experimental data to predict the adsorption kinetics of nickel onto cation resin.

3.8.1. The pseudo-first-order equation

The Lagergren's rate equation [63] is one of the most widely used rate equation to describe the adsorption of an adsorbate from the liquid phase. The linear form of pseudo-first-order equation is given as:

$$\log(q_{\mathrm{e}}-q_t)=\log q_{\mathrm{e}}-\frac{k_1}{2.303}t \tag{18}$$

where q_t (mg/g) is the amount of nickel ions adsorbed at time t and k_1 (min^{-1}) is the rate constant of the pseudo-first-order adsorption model. The experimental results of the first-order rate constants were presented in Table 3. The adsorption data have a high regression coefficient which suggests that the adsorption of Ni^{2+} ions on cation resin follows entirely the pseudo-first-order adsorption kinetics.

Table 2
The best-fit isotherm models to the experimental equilibrium data by several different error functions

Isotherm model	HYBRID	ARE	EABS	MPSD
Langmuir	5.01869	3.0112	1.07152	33.48138
Freundlich	5.03482	3.02089	1.04358	31.35125
Temkin	4.98028	2.988169	1.074278	37.38014
Elovich	13.64081	8.18448	3.122054	112.3237
Fowler–Guggenheim	83.25910123	49.95546074	17.50883022	522.5302909
Kiselev	96.58427	57.95056	20.44965	607.9397
Hill–de Boer	83.3128	49.98768	17.52023	522.8569
Jovanovic	126.33717	75.802	25.631	675.8244
Hill	4.8889	2.933316	1.01184	31.29835
Koble–Corrigan	169.6496	101.7898	34.61513	920.1112

3.8.2. The pseudo-second-order rate equation

The pseudo-second-order kinetic model is based on the assumption that chemisorption is the rate-determining step and is given as [64]:

$$\frac{t}{q_t} = \frac{1}{k_2 q_e^2} + \frac{t}{q_e} \tag{19}$$

where k_2 (g/(mg min)) is the rate constant of the pseudo-second-order kinetic model. The relationship did not show a good compliance with the pseudo-second-order equation.

The correlation coefficient for the linear plot, R^2, suggests a poor relationship between the parameters and also explained that the process of adsorption did not fit pseudo-second-order kinetic model (Table 3).

3.8.3. Elovich model

The Elovich equation was first developed to describe the kinetics of chemisorption of gas unto solids [65]. The linear form of the Elovich equation is presented by the following equation:

$$q_t = \frac{1}{\beta}\ln(\alpha\beta) + \frac{1}{\beta}\ln(t) \tag{20}$$

Table 3
Kinetic rate constants related to the sorption of Ni^{2+} ions onto cation-exchange resin

Kinetic model	Kinetic rate constants	R^2
Pseudo-first-order	$k_1 = 0.0605689$	0.8413
Pseudo-second-order	$k_2 = 0.00251$	0.6095
Elovich model	$\alpha = 0.8367$ $\beta = 0.26388$	0.8978

where α is the initial sorption rate constant (mg/g min) and the parameter β is related to the extent of surface coverage and the activation energy for chemisorption (g/mg). The constants α and β were obtained from the slope and intercept of the linear plot of q_t vs. $\ln t$ and the values were presented in Table 3. The correlation coefficient of Ni^{2+} ions was 0.8978 which is better than that of both the pseudo-first- and pseudo-second-order models.

The nonlinearized kinetic diffusion equations with experimental data are shown in Fig. 6.

3.9. Adsorption mechanism

Diffusion models were also employed to describe the nickel adsorption process. Three main steps are involved in the solid–liquid sorption process between the metal ions and the adsorbent [66]; (a) the metal ions are transferred from the bulk solution to the external surface of the adsorbent. This is known as film diffusion, (b) the metal ions are transferred within the pores of the adsorbent. This is known as intra-particle diffusion, occurring either as pore diffusion or as a solid surface diffusion mechanism, and (c) the active sites on the surface of the adsorbent capture the metal ions.

3.9.1. The intra-particle diffusion model

The intra-particle diffusion model is given by the following equation [67]:

$$q_t = k_{int}\, t^{1/2} + C \tag{21}$$

where k_{int} is the intra-particle diffusion rate constant (mg/(g min)),The intra-particle diffusion plots of the experimental results, and C is a constant that gives an

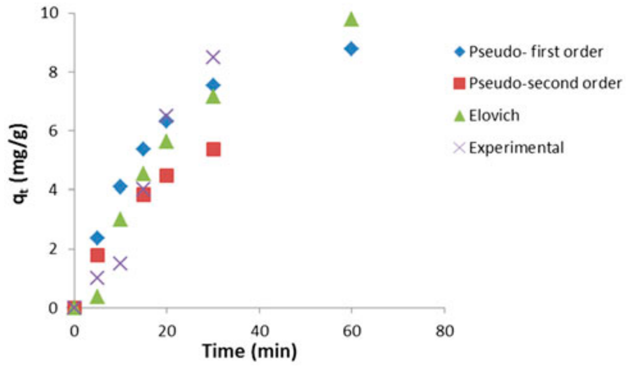

Fig. 6. Comparison of experimental and predicted kinetics of nickel ions onto cation-exchange resin.

Table 4
Diffusion coefficients for Ni^{2+} ions sorption onto cation-exchange resin

Adsorption mechanism	Diffusion constants	R^2
Intra-particle diffusion model	$k_{int} = 0.6114$ $C = -0.4929$	0.9614
Liquid film diffusion	$R' = 0.0962$	0.8814

idea about the boundary layer thickness (mg/g). A plot of q_t vs. $t^{1/2}$ should be a straight line with a slope k_{int} when the intra-particle diffusion is the sole rate-limiting step. However, it is not always the case, and adsorption kinetics may be controlled by film diffusion and intra-particle diffusion simultaneously. The values of k_{int}, C, and correlation coefficient (R^2) obtained from intra-particle diffusion plots were 0.6114, –0.4929, and 0.9614, respectively, as shown in Table 4. The values of C obtained from intra-particle diffusion model indicated that intra-particle diffusion may not be the controlling factor in determining the kinetics of the process, and film diffusion controls the initial rate of the adsorption, it also indicated the thickness of the boundary layer.

According to Michelson et al. [68], if pore diffusion was to be the rate limiting, the pore diffusion coefficient, D_p, should be in the range from 10^{-11} to 10^{-13} cm^2/s.

The pore diffusion coefficient (D_p) is calculated by the following equation:

$$t_{1/2} = \frac{0.03\, r_0^2}{D_p} \tag{22}$$

where r_0 is radius of the sorbent (cm), D_p is pore diffusion coefficient (cm^2/sec), and $t_{1/2}$ is the time for half change (sec). It was found that $D_p = 1.752 \times 10^{-13}$ cm^2/sec which is in the range from 10^{-11} to 10^{-13} cm^2/s, indicating that intra-particle diffusion is controlling step.

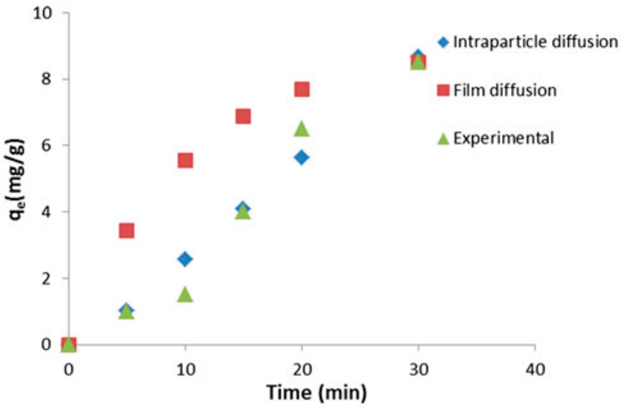

Fig. 7. Comparison of experimental and predicted mechanism of nickel ions onto cation-exchange resin.

3.9.2. Liquid film diffusion model

The film diffusion mass transfer rate equation presented by Boyd et al. [69] is:

$$\ln\left(1 - \frac{q_t}{q_e}\right) = -R't \tag{23}$$

$$R' = \frac{3D_e}{r_o\, \Delta r_o k'} \tag{24}$$

where R´ (min^{-1}) is liquid film diffusion constant, D_e' (cm^2/min) is effective liquid film diffusion coefficient, r_o (cm) is radius of adsorbent beads, Δr_0 (cm) is the thickness of liquid film, and $k´$ is equilibrium constant of adsorption.

A plot of $\ln(1 - q_t/q_e)$ vs. t should be a straight line with a slope $-R´$ if the film diffusion is the rate-limiting step. As shown from Table 4, $R^2 = 0.8814$, which indicated that Ni^{2+} adsorption is governed by film diffusion process in the initial stages of adsorption then intra-particle diffusion.

Table 5
Diffusion coefficients for Ni^{2+} sorption onto cation-exchange resin

Film Diffusion coefficient (cm^2/s)	Pore diffusion coefficient (cm^2/s)
1.482×10^{-12}	1.752×10^{-13}

According to Michelson et al. [68] for film diffusion to be rate-determining step, the value of the film diffusion coefficient, D_f, should be in the range from 10^{-6} to 10^{-8} cm^2/s.

The film diffusion coefficient, D_f is calculated by the following equation:

$$t_{1/2} = \frac{0.23 \times r_o \times \Delta r_o}{D_f} \times \left(\frac{C^-}{C}\right) \tag{25}$$

where $(C^-/C)$is the equilibrium loading of the adsorbent. It was found that $D_f = 1.482 \times 10^{-12}$ cm^2/s, which is not in the range from 10^{-6} to 10^{-8} cm^2/s indicating that film diffusion is not the controlling step.

The nonlinearized diffusion equations with experimental data are shown in Fig. 7. The values of film and pore diffusion coefficients are shown in Table 5.

4. Conclusions

A strong cation-exchange resin (IR 120 H) was successfully utilized for the removal of Ni^{2+} ions from aqueous solution by batch adsorption method. The adsorption process was found to be dependent on many factors such as the initial concentration of metal ion, contact time, adsorbent dose, and stirring speed. The percentage removal of nickel ion increased with increasing contact time, adsorbent dose, and stirring speed. On the other hand, increasing initial metal ion concentration decreased the percentage removal of nickel ion. Optimum removal of nickel ions was obtained at a contact time of 40 min, initial nickel ion concentration of 500 ppm, adsorbent dose of 4 gm/100 ml, the solution pH 5, and stirring speed of 250 rpm. The equilibrium data were tested using the Langmuir, Freundlich, Temkin, Elovich, Fowler-Guggenheim, Kiselev, Hill-de Boer, Jovanovic, Hill, and Koble-Corrigan isotherms. Correlation coefficients indicated the following order to fit isotherms: Langmuir > Koble–Corrigan > Freundlich > Hill > Jovanovic > Temkin > Hill–de Boer > Fowler–Guggenheim > Kiselev > Elovich. On the basis of the lowest values of the four error functions studied, Hill model presented the best correlation for the experimental data. Kinetic parameters were also analyzed using the pseudo-first-order, pseudo-second-order, and Elovich model. Intra-particle diffusion model and the liquid film diffusion model were used to investigate the adsorption mechanism. Kinetic studies showed that the adsorption of Ni^{2+} ions onto ion-exchange resin followed Elovich kinetic model, and indicates that the intra-particle diffusion controls the rate of adsorption.

List of symbols

a — Koble–Corrigan parameter (L^n mg^{1-n}/g)
A_T — Temkin isotherm equilibrium binding constant (L/mg)
b — Koble–Corrigan parameter
b_T — Temkin isotherm (–)
B — heat of sorption constant (J/mol)
C — constant related to boundary layer thickness (mg/g)
C_o — equilibrium nickel concentration (mg/L)
D'_e — effective liquid film diffusion (cm^2/min)
D_f — film diffusion coefficient (cm^2/s)
D_P — pore diffusion coefficient (cm^2/s)
k' — equilibrium constant of adsorption
k_1 — rate constant of the pseudo-first-order (min^{-1})
k_2 — rate constant of the pseudo-first-order (g/mg min)
k_n — constant of complex formation between adsorbed molecules
K_D — Hill constant
K_E — Elovich equilibrium constant (L/mg)
K_F — Freundlich adsorption capacity constant (mg/g) (mg/L)$^{1/n}$
K_{FG} — Fowler–Guggenheim equilibrium constant (L/mg)
K_{1H} — Hill–de Boer constant L/mg
K_{in} — intra-particle diffusion constant
K_j — Jovanovic isotherm constant (L/mg)
K_{1K} — Kiselev equilibrium constant (L/mg)
K_2 — energetic constant of the interaction between adsorbed molecule (J/mol)
K_L — Langmuir isotherm constant (L/mg)
M — mass of adsorbent (g)
n — number of data points (–)
n_f — Freundlich adsorption intensity constant (–)
n_H — Hill cooperativity coefficient of the binding interaction (–)
$n(k–c)$ — Koble–Corrigan parameter
P — number of parameters
q_e — amount of nickel adsorbed at equilibrium (mg/g)
$q_{e,i,cal}$ — amount of calculated adsorbed nickel at equilibrium (mg/g)
$q_{e,i,meas}$ — amount of measured adsorbed nickel at equilibrium (mg/g)
q_m — maximum monolayer adsorption capacity (mg/g)

q_{SH} — Hill isotherm maximum uptake saturation (mg/L)
q_t — amount of nickel adsorbed at time (t) (mg/g)
R_{o} — radius of adsorbent beads (cm)
Δr_{o} — thickness of liquid film (cm)
R — universal gas constant (J/mol K)
R' — liquid film diffusion constant (min^{-1})
R_{L} — separation factor
t — time (min)
T — temperature (K)
$t_{1/2}$ — time for half change (s)
V — volume of solution (L)
W — interaction energy between adsorbed molecules (KJ/mol)

Greek

α — initial sorption rate constant (mg/g min)
β — extent of surface coverage and activation energy for chemisorptions (g/mg)
θ — degree of surface coverage of adsorbent surface
θ_{H} — fractional coverage

References

[1] R.F. Weiner, R. Matthews, Environmental Engineering, Butterworth-Heinemann, United Kingdom, 2003, p. 102.

[2] Y. Bulut, Z. Tez, Removal of heavy metals from aqueous solution by sawdust adsorption, J. Environ. Sci. 19 (2007) 160–166.

[3] M.N. Zafar, R. Nadeem, M.A. Hanif, Biosorption of nickel from protonated rice bran, J. Hazard. Mater. 143 (2007) 478–485.

[4] M. Cempel, G. Nikel, Nickel: A review of its sources and environmental toxicology, Polish J. Environ. Stud. 15 (2006) 375–382.

[5] R.S. Dave, G.B. Dave, V.P. Mishra, Removal of nickel from electroplating wastewater by weakly basic chelating anion exchange resins: DOWEX 50x4, DOWEX 50x2 and DOWEX M-4195, J. Appl. Sci. Environ. Sanit. 6 (2011) 39–44.

[6] K. Dermentzis, A. Christoforidis, E. Valsamidou, Removal of nickel, copper, zinc and chromium from synthetic and industrial wastewater by electrocoagulation, Int. J. Environ. Sci. 1 (2011) 697–710.

[7] K. Trivunac, S. Stevanovic, Removal of heavy metal ions from water by complexation-assisted ultrafiltration, Chemosphere 64 (2006) 486–491.

[8] B.V. Tangahu, S.R.S. Abdullah, H. Basri, M. Idris, N. Anuar, M. Mukhlisin, A Review on heavy metals (As, Pb, and Hg) uptake by plants through phytoremediation, Int. J. Chem. Eng. 15 (2011) 814–826.

[9] W. Ma, P. Zong, Z. Cheng, B. Wang, B. Wang, Q. Sun, Adsorption and bio-sorption of nickel ions and reuse for 2-chlorophenol catalytic ozonation oxidation degradation from water, J. Hazard. Mater. 266 (2014) 19–25.

[10] F.A. Dawodu, K.G. Akpomie, Simultaneous adsorption of Ni(II) and Mn(II) ions from aqueous solution unto a Nigerian kaolinite clay, J. Mater. Res. Technol. 3 (2014) 129–141.

[11] N. Gupta, A.K. Kushwaha, M.C. Chattopadhyaya, Adsorptive removal of Pb^{2+}, Co^{2+} and Ni^{2+} by hydroxyapatite/chitosan composite from aqueous solution, J. Taiwan. Inst. Chem. E. 43 (2012) 125–131.

[12] L.Y. Lee, X.J. Lee, P.C. Chia, K.W. Tan, S. Gan, Utilisation of *Cymbopogon citratus* (lemon grass) as biosorbent for the sequestration of nickel ions from aqueous solution: Equilibrium, kinetic, thermodynamics and mechanism studies, J. Taiwan Inst. Chem. Eng. 45 (2014) 1764–1772.

[13] R.M. Kulkarni, K.V. Shetty, G. Srinikethan, Cadmium (II) and nickel (II) biosorption by *Bacillus laterosporus* (MTCC 1628), J. Taiwan Inst. Chem. Eng. 45 (2014) 1628–1635.

[14] P.S. Kumar, S. Ramalingam, S.D. Kirupha, A. Murugesan, T. Vidhyadevi, S. Sivanesan, Adsorption behavior of nickel(II) onto cashew nut shell: Equilibrium, thermodynamics, kinetics, mechanism and process design, Chem. Eng. J. 167 (2011) 122–131.

[15] M. El-Sadaawy, O. Abdelwahab, Adsorptive removal of nickel from aqueous solutions by activated carbons from doum seed (*Hyphaenethebaica*) coat Alexandria Eng. J. 53 (2014) 399–408

[16] H. Hasar, Adsorption of nickel(II) from aqueous solution onto activated carbon prepared from almond husk, J. Hazard. Mater. 97 (2003) 49–57.

[17] A. Kurniawan, A.N. Kosasih, J. Febrianto, Y.-H. Ju, J. Sunarso, N. Indraswati, S. Ismadji, Evaluation of cassava peel waste as lowcost biosorbent for Ni-sorption: Equilibrium, kinetics, thermodynamics and mechanism, Chem. Eng. J. 172 (2011) 158–166.

[18] D. Harikishore Kumar Reddy, D.K.V. Ramana, K. Seshaiah, A.V.R. Reddy, Biosorption of Ni(II) from aqueous phase by *Moringa oleifera* bark, a low cost biosorbent, Desalination 268 (2011) 150–157.

[19] N.H. Shaidan, U. Eldemerdash, S. Awad, Removal of Ni(II) ions from aqueous solutions using fixed-bed ion exchange column technique, J. Taiwan Inst. Chem. Eng. 43 (2012) 40–45.

[20] M.E. Argun, Use of clinoptilolite for the removal of nickel ions from water: Kinetics and thermodynamics, J. Hazard. Mater. 150 (2008) 587–595.

[21] T. Mahmood, M.T. Saddique, A. Naeem, S. Mustafa, B. Dilara, Z.A. Raza, Cation exchange removal of Cd from aqueous solution by NiO, J. Hazard. Mater. 185 (2011) 824–828.

[22] K.Y. Foo, B.H. Hameed, Insights into the modeling of adsorption isotherm systems, Chem. Eng. J. 156 (2010) 2–10.

[23] H.S. Ibrahim, T.S. Jamil, E.Z. Hegazy, Application of zeolite prepared from Egyptian kaolin for the removal of heavy metals: II. Isotherm models, J. Hazard. Mater. 182 (2010) 842–847.

[24] B. Alyüz, S. Veli, Kinetics and equilibrium studies for the removal of nickel and zinc from aqueous solutions by ion exchange resins, J. Hazard. Mater. 167 (2009) 482–488.

[25] M.M. Montazer-Rahmati, P.P. Rabbani, A. Abdolali, A.R. Keshtkar, Kinetics and equilibrium studies on biosorption of cadmium, lead, and nickel ions from aqueous solutions by intact and chemically modified brown algae, J. Hazard. Mater. 185 (2011) 401–407.

[26] S. Malamisand, E. Katsou, A review on zinc and nickel adsorption on natural and modified zeolite, bentonite and vermiculite: Examination of process parameters, kinetics and isotherms, J. Hazard. Mater. 252–253 (2013) 428–461.

[27] A. Deepatana, M. Valix, Comparative adsorption isotherms and modeling of nickel and cobalt citrate complexes onto chelating resins, Desalination 218 (2008) 334–342.

[28] Y.S. Ho, J.F. Porter, G. McKay, Equilibrium isotherm studies for the sorption of divalent metal ions onto peat: Copper, nickel and lead single component systems, Water Air Soil Pollut. 141 (2002) 1–33.

[29] S. Rangabhashiyam, N. Anu, M.S.G. Nandagopal, N. Selvaraju, Relevance of isotherm models in biosorption of pollutants by agricultural byproducts, J. Environ. Chem. Eng. 2 (2014) 398–414.

[30] K. Vijayaraghavan, T.V.N. Padmesh, K. Palanivelu, M. Velan, Biosorption of nickel(II) ions onto *Sargassum wightii*: Application of two-parameter and three-parameter isotherm models, J. Hazard. Mater. 133 (2006) 304–308.

[31] O. Hamdaoui, E. Naffrechoux, Modeling of adsorption isotherms of phenol and chlorophenols onto granular activated carbonPart I. Two-parameter models and equations allowing determination of thermodynamic parameters, J. Hazard. Mater. 147 (2007) 381–394.

[32] Z. Benmaamar, A. Bengueddach, Correlation with different models for adsorption isotherms of m-xylene and toluene on zeolites, J. Appl. Sci. Environ. Sanit. 2 (2007) 43–56.

[33] H. Qiu, L. LV, B. Pan, Q. Zhang, W. Zhang, Q. Zhang, Critical review in adsorption kinetic models, J. Zhejiang Univ. Sci. A, 10 (2009) 716–724.

[34] Z. Chen, W. Ma, M. Han, Biosorption of nickel and copper onto treated alga (*Undaria pinnatifida*): Application of isotherm and kinetic models, J. Hazard. Mater. 155 (2008) 327–333.

[35] S. Rengaraj, J.W. Yeon, Y. Kim, Y. Jung, Y. Ha, W.H. Kim, Adsorption characteristics of Cu(II) onto ion exchange resins 252H and 1500H: Kinetics, isotherms and error analysis, J. Hazard. Mater. 143 (2007) 469–477.

[36] E. Malkoc, Ni(II) removal from aqueous solutions using cone biomass of *Thuja orientalis*, J. Hazard. Mater. 137 (2006) 899–908.

[37] G. Rani, M. Harapriya, Microbial biomass: An economical alternative for removal of heavy metals from waste water, Indian J. Exp. Biol. 41 (2003) 945–966.

[38] S. Rengaraj, C.K. Joo, Y. Kim, J. Yi, Kinetics of removal of chromium from water and electronic process wastewater by ion exchange resins: 1200H, 1500H and IRN97H, J. Hazard. Mater. 102 (2003) 257–275.

[39] B.A. Fil, R. Boncukcuoglu, A.E. Yilmaz, S. Bayar, Adsorption kinetics and isotherms for the removal of zinc ions from aqueous solutions by an ion-exchange resin, J. Chem. Soc. Pak. 34 (2012) 841–848.

[40] Z. Reddad, C. Gerente, Y. Andres, Pierre Le Cloirec, Adsorption of several metal ions onto a low -cost biosorbents: Kinetics, equilibrium studies, Environ. Sci. Technol. 36 (2002) 2067–2074.

[41] J. Vaghetti, E. Lima, B. Royer, J. Brasil, B. da Cunha, N. Simon, Application of Brazilian-pine fruit coat as a biosorbent for removal of Cr (VI) from aqueous solution-kinetic and equilibrium study, Biochem. Eng. J. 42 (2008) 67–76.

[42] I. Langmuir, The adsorption of gases on plane surfaces of glass, mica and platinum, J. Am. Chem. Soc. 40 (1918) 1361–1403

[43] K.R. Hall, L.C. Eagleton, A. Acrivos, T. Vermeulen, Pore- and solid-diffusion kinetics in fixed-bed adsorption under constant-pattern conditions, Ind. Eng. Chem. Fundam. 5 (1966) 212–223.

[44] H.M. Freundlich, Over the adsorption in solution, Z. Phys Chem. 57 (1906) 385–470.

[45] F. Slejko, Adsorption Technology: A Step by Step Approach to Process, Eva Appl Marcel Dekker, New York, NY, 1985.

[46] Z. Chen, W. Ma, M. Han, Biosorption of nickel and copper onto treated alga (*Undaria pinnatifida*): Application of isotherm and kinetic models, J. Hazard. Mater. 155 (2008) 327–333.

[47] M. Temkin, V. Pyzhev, Kinetics of ammonia synthesis on promoted ion catalyst, Acta Physicochem. URSS 12 (1920) 217–222.

[48] S.Y. Elovich, O.G. Larinov, Theory of adsorption from solutions of nonelectrolytes on solid (I) equation adsorption from solutions and the analysis of its simplest form, (II) verification of the equation of adsorption isotherm from solutions, Izv. Akad. Nauk. SSSR, Otd. Khim. Nauk. 2 (1962) 209–216

[49] R.H. Fowler, E.A. Guggenheim, Statistical Thermodynamics, Cambridge University Press, London, 1939, pp. 431–450.

[50] A.V. Kiselev, Vapor adsorption in the formation of adsorbate molecule complexes on the surface, Kolloid Zhur. 20 (1958) 338–348.

[51] T.L. Hill, Statistical mechanics of multimolecular adsorption II. Localized and mobile adsorption and absorption, J. Chem. Phys. 14 (1946) 441.

[52] J.H. de Boer, The Dynamical Character of Adsorption, Oxford University Press, Oxford, 1953.

[53] D.S. Jovanovic, Physical adsorption of gases. I: Isotherms for monolayer and multilayer adsorption, Colloid. Polym. Sci. 235 (1969) 1203–1214.

[54] A.V. Hill, The possible effects of the aggregation of the molecules of haemoglobin on its dissociation curves, J. Physiol. 40 (1910) 4–7.

[55] L.K. Koopal, W.H. van Riemsdijk, J.C.M. de Wit, M.F. Benedetti, Analytical isotherm equation for multicomponent adsorption to heterogeneous surfaces, J. Colloid Interface Sci. 166 (1994) 51–60.

[56] D. Ringot, B. Lerzy, K. Chaplain, J.P. Bonhoure, E. Auclair, Y. Larondelle, In vitro biosorption of ochratoxin A on the yeast industry by-products: Comparison of isotherm models, Bioresour. Technol. 98 (2007) 1812–1821.

[57] R.A. Koble, T.E. Corrigan, Adsorption isotherm for pure hydrocarbons, Ind. Eng. Chem. 44 (1952) 383–387.

[58] R. Han, J. Zhang, P. Han, Y. Wang, Z. Zhao, M. Tang, Study of equilibrium, kinetic and thermodynamic parameters about methylene blue adsorption onto natural zeolite, Chem. Eng. J. 145 (2009) 496–504.

[59] J.F. Porter, G. McKay, K.H. Choy, The prediction of sorption from a binary mixture of acidic dyes using single and mixed isotherm variants of the ideal adsorbed solute theory, Chem. Eng. Sci. 54 (1999) 5863–5885.

[60] A. Kapoor, R.T. Yang, Correlation of equilibrium adsorption data of condensible vapours on porous adsorbents, Gas Sep. Purif. 3 (1989) 187–192.

[61] D.W. Marquardt, An algorithm for least-squares estimation of nonlinear parameters, J. Soc. Ind. Appl. Math. 11 (1963) 431–441.

[62] A. Seidel, D. Gelbin, On applying the ideal adsorbed solution theory to multicomponent adsorption equilibria of dissolved organic components on activated carbon, Chem. Eng. Sci. 43 (1988) 79–89.

[63] Y.S. Ho, G. McKay, Kinetic models for the sorption of dye from aqueous solution by wood, J. Environ. Sci. Health 76 (1998) 183–191.

[64] Y.S. Ho, G. Mckay, The kinetics of sorption of basic dyes from aqueous solution by sphagnum moss peat, Can. J. Chem. Eng. 76 (1998) 7–822.

[65] M. Low, Kinetics of chemisorptions of gases on solids, Chem. Rev. 60 (1960) 267–312.

[66] M.H. Kalavathy, T. Karthikeyan, S. Rajgopal, L.R. Miranda, Kinetic and isotherm studies of Cu (II) adsorption onto H_3PO_4, J. Colloid Interface Sci. 292 (2005) 354–362.

[67] W.J. Weber Jr., J.C. Morriss, Kinetics of adsorption on carbon from solution, J. Sanitary Eng. 89 (1963) 31–60.

[68] L.D. Michelson, P.G. Gideon. E.G. Pace, L.H. Kutal, US Department Industry, Office of Water Research and Technology, Bulletin, 74, 1975.

[69] G.E. Boyd, A.W. Adamson, L.S. Myers, The exchange adsorption of ions from aqueous solutions by organic zeolites, II, Kinetics, J. Am. Chem. Soc. 69 (1947) 2836–2848.